Nanoscale

PAPER

View Article Online
View Journal | View Issue

Cite this: *Nanoscale*, 2014, **6**, 6997

Sub-diffraction positioning of a two-photon excited and optically trapped quantum dot†

Liselotte Jauffred,[a] Anders Kyrsting,[a] Eva C. Arnspang,[b] S. Nader S. Reihani‡[a] and Lene B. Oddershede*[a]

Received 10th March 2014
Accepted 4th May 2014

DOI: 10.1039/c4nr01319k

www.rsc.org/nanoscale

Colloidal quantum dots are luminescent long-lived probes that can be two-photon excited and manipulated by a single laser beam. Therefore, quantum dots can be used for simultaneous single molecule visualization and force manipulation using an infra-red laser. Here, we show that even a single optically trapped quantum dot, performing restricted Brownian motion within the focal volume, can be two-photon excited by the trapping laser beam and its luminescence can be detected by a camera. After two-photon excitation for a time long enough, the emitted light from the quantum dot is shown to blueshift. A quantum dot is much smaller than a diffraction limited laser focus and by mapping out the intensity of the focal volume and overlaying this with the positions visited by a quantum dot, a quantum dot is shown often to explore regions of the focal volume where the intensity is too low to render two-photon absorption likely. This is in accordance with the observation that a trapped quantum dot is only fluorescing 5–10 percent of the time. The results are important for realizing nano-scale quantum dot control and visualization and for correct interpretation of experiments using two-photon excited quantum dots as markers.

Introduction

Due to their high luminescence and low photobleaching, colloidal quantum dots (QDs) have proven extremely useful as fluorescent markers of single molecules[1–3] and have been used to monitor, *e.g.*, binding of a single protein to DNA[4,5] and of a bacteriophage to a cell.[6] With commercially available QDs the toxicity is low[7] and several molecular motors have proven to retain activity though bioconjugated to a colloidal QD.[5,8–12] In the study of molecular motors, it is useful not only to follow the path of the motor but also to investigate the force with which the motor is acting. QDs are excellent for this purpose, as they can serve as handles for force-manipulation techniques.[13] Also, aggregates of colloidal QDs have been shown to be two-photon excitable by an NIR laser,[14] and semiconductor nanorods can be simultaneously rotated and two-photon excited.[15] Hence, a QD can simultaneously be used as a handle for manipulation, for force-spectroscopy, and as a luminescent marker.

Large intensity gradients are present in a laser focus, and in practice, it is unavoidable to also have spherical aberration. This, however, can be eliminated to a high degree, for instance by changing the tube length,[16] the immersion media,[17,18] or by active feed-back mechanisms using a Spatial Light Modulator (SLM).[19] Two-photon excitation of a QD requires high photon density, and only a minor part of a typical diffraction limited laser focus will be intense enough to render QD excitation likely. Probably for this reason, the emission from a two-photon excited individual trapped QD was never before detected.

As the size of a diffraction limited spot is below the resolution of conventional microscopy, it is not trivial to map out the exact intensity distribution within the focus nor to determine where in the focus a nanoparticle is stably trapped. By translating a fluorescent layer through a focused laser spot the 3D intensity distribution can be deducted *via* the bleaching of the layer by the trapping laser.[18] This methodology, combined with optical trapping of gold and polystyrene particles, recently showed that certain sizes of metallic nanoparticles stably trap in front of the focus.[18] Apart from being of fundamental interest, the question of exactly where a nanoparticle is localized also has importance for reliable positioning on the nanometer scale, *e.g.*, for manipulation of proteins on a filament or for nano-architectural purposes.

Here, we visualize a QD that is two-photon excited and constrained only by an infrared laser. The QD performs significant thermal fluctuations within the optical trap and therefore, it only rarely explores the parts of the focal volume with

[a]*The Niels Bohr Institute, University of Copenhagen, Denmark. E-mail: oddershede@nbi.dk*

[b]*MEMPHYS, University of Southern Denmark, Odense, Denmark*

† Electronic supplementary information (ESI) available: Fig. S1: blue shift of emission from a two-photon excited quantum dot. Fig. S2: corner frequency and spring constant *versus* laser power for the three translational directions. Fig. S3: accumulated probability for QD localization, excitation, and emission detection as a function of focal intensity. See DOI: 10.1039/c4nr01319k

‡ Present address: Sharif University, Tehran, Iran.

intensities high enough to render two-photon excitation likely. This is proven by mapping out the 3D intensity distribution within the laser focus and by overlaying this with positions visited by the optically trapped QD. Hence, we find that the trapping volume is significantly larger than the two-photon excitation volume.

Methodology

The QDs used were water-soluble streptavidin-coated sAv-Qdot 655 and Qdot 655-NH2 (Invitrogen). The QDs were diluted in a 50 mM sodium borate (pH 8.2) solution with 1% (w/v) BSA at room temperature (293 K) to maximize stabilization and minimize aggregation. The QD stock solutions were diluted from $1/10^3$ to $1/10^5$ before usage and filtered (0.5 μm pore size) to remove larger aggregates.

Optical trapping

The QDs were trapped and two-photon excited by a Nd:YVO_4 laser (5 W Spectra Physics BL, 1064 nm, TEM_{00}). The laser was implemented in an inverted Leica confocal SP5 microscope and focused to a diffraction limited spot by an oil immersion objective (Leica HCX PL APO 100X NA = 1.4 oil CS). To minimize spherical aberration and hence maximize the strength of the trap in the axial direction we used an immersion oil with a refractive index of $n = 1.538$ (Cargille), which is optimal for cover glasses with thickness # 1.5 while trapping at a depth of 5 μm.[17] In all parts of the experiments care was taken to have only a single QD in the trap. If a second QD entered the trap, or if the trapped object appeared to be an aggregate (with increased fluorescence), this part of the data was excluded from the analysis.

For all trapping experiments we used laser powers in the range from 1.4 W to 3.7 W (measured at the exit of the laser). This corresponds to powers in the sample of 250 mW to 800 mW. However, QDs can be two-photon excited with laser powers below 200 mW.[14]

Imaging

A Hg lamp and filtercubes, as detailed in ref. 13 and 14, were used to navigate in the sample prior to measurements. To enable visualization of the trapped and two-photon excited QD we fine tuned the telescope lenses controlling the axial position of the trap, so that the focus of the objective would exactly equal the axial equilibrium position of the optical trap. QDs are known to perform a blueshift in their emission upon extensive linear excitation.[20] In order to detect spectral instabilities and dynamics we inserted a QuadView image splitter. This had dichromatic mirrors at Q585LP, Q630LP and Q690LP nm and with D565/40, D605/20, and D655/20 fluorescence emission bandpass filters (Chroma Technology, Rockingham, VT). The QuadView image splitter was designed for simultaneous detection of QDs at different wavelengths. To block light from the 1064 exciting IR laser we used a combination of hot mirrors (FM01, Thorlabs) and a colored glass filter (FGS900, Thorlabs). The photoluminescence of the QDs were detected with a cooled EMCCD (Andor, Ixon). In the experiment where a QD stuck to the surface was two-photon excited (Fig. 2a and b) the surface was axially displaced in order to achieve the highest detection signal on the EMCCD. As the QD fluorescence lifetime is on the order of tens of ns (ref. 21) and our sampling time was 100 ms we were averaging over many blinking intermittencies using the EMCCD.

Mapping of focal intensity distribution

We determined the intensity distribution in the focal region by translating a 10 nm thin fluorescent film (BSA with Alexa 555) through the 1064 nm laser focus in small steps by using a telescope whose focus was decoupled from that of the microscope objective. The geometry of the laser-bleached regions gave information on the focal intensity and a 3D map could be made, more details on the mapping method are given in ref. 18.

Sub-diffraction tracking of a QD

We trapped individual QDs approximately 5 μm from the surface. To track the positions visited by a trapped QD in three dimensions, regardless of whether the QD was emitting light or not, we used a quadrant photodiode (QPD, S5981, Hamamatsu) inserted in the back focal plane as described in ref. 13 and 14. The time resolution of the QPD measurements was 45 μs (22 kHz sampling frequency). We filtered our data on the basis of the raw QPD signal: the voltage signal on the QPD had a typical amplitude when a single QD was in the trap. When more QDs entered the trap, this voltage amplitude increased. This was immediately visible from the on-the-fly power spectral analysis by a shift in f_c. In this manner, we ensured that all time series analyzed was from the trapping of a single QD.

Results and discussion

To visualize a trapped QD two types of experiments were performed with the setup sketched in Fig. 1. In the first experiment the streptavidin-coated QD was unspecifically attached to a coverslip surface and the trap was positioned exactly at the QD, thus exciting the QD as sketched in Fig. 2a. The corresponding emitted intensity as a function of time is shown in Fig. 2b. Clearly, the intensity of the optical trap was high enough to excite the immobilized QD by two-photon absorption and the emitted light performs a blinking behavior that is characteristic of an individual QD.[22] The recorded signal in this type of experiment was somewhat sensitive to drift of the sample with respect to the focus of the optical trap, therefore, care was taken only to analyze time series without drift.

When a QD was irradiated for a long enough time interval, a blueshift of the light emitted by the two-photon excited QD was observed. This spectral shift is shown in the images in Fig. 1b, the emission wavelength decreased from 655 nm to 605 nm after ~40–60 seconds of irradiation as visible from the long time series shown in Fig. S1.† This result is novel for two-photon excited QDs but in accordance with recent observations for linearly excited QDs which were observed to undergo a continuous blueshift before reaching the ionized dark state.[20]

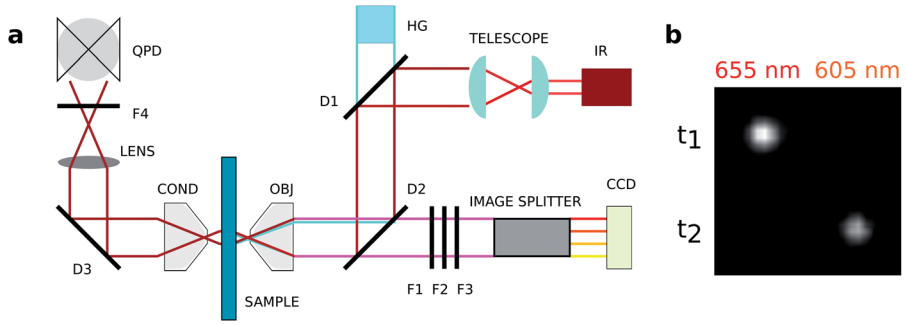

Fig. 1 (a) Schematic of the experimental setup. The 1064 nm trapping laser beam (IR) is expanded by a telescope and deflected by two dichroic mirrors (D1, D2) before it enters the sample trough the objective (OBJ) of an inverted Leica SP5 microscope. The positions visited by the trapped object are measured by a quadrant photodiode (QPD) using the forward scattered light that is collected by the condenser (COND) and deflected by a dichroic mirror (D3). A lens focuses the forward scattered light onto the QPD and a filter (F4) reduces the intensity. Excitation light from a mercury lamp (HG) facilitates navigation in the sample, but during the experiments the QDs are solely excited by the IR laser beam. The fluorescent emission from a single QD is filtered by two hot mirrors and color filters (F1, F2, F3). Spectral selection is performed with an image splitter and projected onto the sensitive EMCCD. (b) Snapshots at two different times (t_1 and t_2) of an immobilized QD blue-shifting from an emission wavelength of (655 ± 20) nm to (605 ± 20) nm.

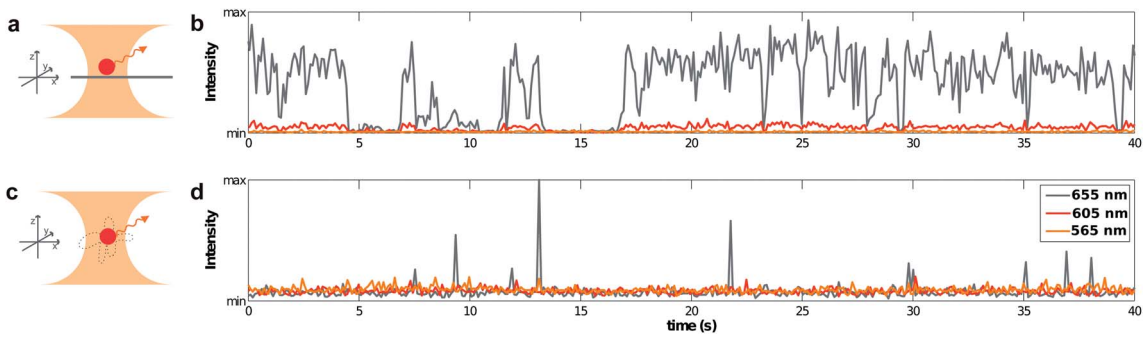

Fig. 2 Two-photon excitation of an immobilized or optically trapped QD. (a) Sketch of the experiment where a QD, adhered to the surface, is two-photon excited by the trapping laser. The sketch is not to scale. (b) Emitted intensity *versus* time from a single QD adhered to the surface. (c) Sketch of the experiment where a QD is optically trapped and two-photon excited in the solution. The QD performs significant thermal fluctuations within the trapping volume; indicated by the punctuated line. The sketch is not to scale. (d) Emitted intensity *versus* time from a single QD optically trapped in solution ~5 μm above the surface. The intensity at different emission wavelengths (655 nm, 605 nm, and 565 nm) are denoted with different colors. A clear signal is only recorded in the 655 nm spectral window but the two other windows (605 nm and 565 nm) are included for comparison.

In the second type of experiment, as sketched in Fig. 2c, a single QD was trapped in solution and two-photon excited by the trapping laser alone. The emitted intensities were recorded and the corresponding time series (one example is shown in Fig. 2d) appear rather different than the recordings from an immobilized QD: only rarely emission from the optically trapped QD was detected by the camera. The reason for the 'spiky' appearance of the emission is most likely a combination of the intrinsic blinking of QD emission and the fact that the trapped QD often explores parts of the trapping volume where the intensity is too low for two-photon excitation of the QD. To resolve this issue, the positions visited by the trapped QDs were also recorded with nanometer resolution in 3D by a quadrant photodiode (QPD). These traces showed that a QD was stably trapped for several minutes, hence ruling out the possibility that the QD left the trap as reported for 24 nm polystyrene beads.[23] In these experiments we did not observe blueshifts of the emission from an optically trapped QD, probably because the thermal fluctuations of the QD caused the integrated excitation time to be rather low.

The QPD measurements gave full information about the 3D trace of a trapped QD and Fig. 3 shows three examples of the positions visited in 3D by an individual QD moving in the trapping potential. The QD depicted in Fig. 3a appears to move within a spherical region and the position histogram is well approximated by a Gaussian function in all three translational directions, thus signifying that the QD experiences a harmonic potential. The position histograms of the QDs depicted in Fig. 3b and c deviate somewhat from Gaussian distributions in all three directions, however, the 'lobes' pointing along the direction of the propagating laser are only sparsely populated, the QD still spends most of its time in the intense center region.

Though efforts were taken to minimize spherical aberration, in practice the focal intensity is never un-aberrated on the nanometer scale and the dynamics of a 12 nm QD moving in a focal region with a width of >500 nm will be heavily influenced

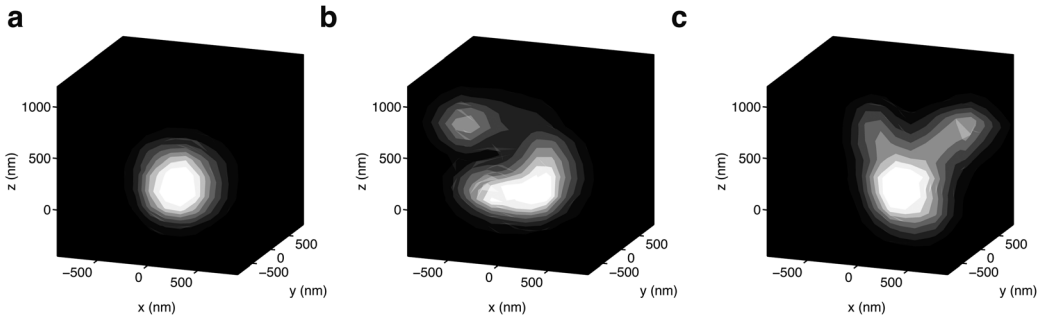

Fig. 3 Three dimensional histograms of the positions visited by three individual colloidal quantum dots (a, b and c) moving in an optical trapping potential where the laser power at the sample was 250 mW. The contours signify percentage of the counts in 10% steps and $z = 0$ nm is set as the mean value of (a).

by the exact focal intensity distribution. Theoretically, the particles are anticipated to be most often trapped at the focal center of the laser beam, however, in practice, the particles are often displaced somewhat away from the center, most pronounced in the axial direction where aberration is significant for high NA objectives. It was recently shown that trapped nanoparticles can be stably trapped both in a position above and in a position below the focus, depending on the particle size and material and the spherical aberration at the focus.[18] Therefore, the exact intensity distribution of the focal region will be decisive for the location of the stable trapping positions of a QD and for where the intensity is large enough to two-photon excite a QD.

To compare the trapping positions with the exact focal intensity distribution we mapped out the focal intensity distribution under the current experimental conditions using the methodologies detailed in ref. 18. The resulting 3D focal intensity distribution is shown in Fig. 4. Cross sections along the white dashed lines in Fig. 4a are shown in Fig. 4b. Clearly, the intensity distribution in the axial direction is not Gaussian but asymmetric with two lobes pointing along the propagation direction of the trapping laser. The strength of the trap was optimized by using a certain immersion media (as detailed in Methods and in ref. 17). However, the fact that the trap is strong does not necessarily imply that the focal intensity distribution is Gaussian. Rather, as the scattering force tends to push trapped objects away from the focus,[18] it might be advantageous to have a sharper intensity gradient at the 'top' of the central intensity cylinder seen in Fig. 4a, especially for trapping an individual QD.

The spherical aberrations and the resulting focal intensity distribution changes considerably when changing the refractive index of the immersion media. A comparison of our mapping with the distributions given for the same oil immersion objective in ref. 18, reveals that spherical aberrations can cause lobes to appear both before or after the laser focus. This rather dramatically change of intensity distributions appear for immersion oils with refractive index in the range from 1.470–1.570.

Interestingly, the lobes visible in the position histogram of Fig. 3b and c resemble the intensity lobes pointing away from the focal region along the propagating laser as visible in Fig. 4. Fig. 5a shows an overlay of the focal intensity (Fig. 4) with the

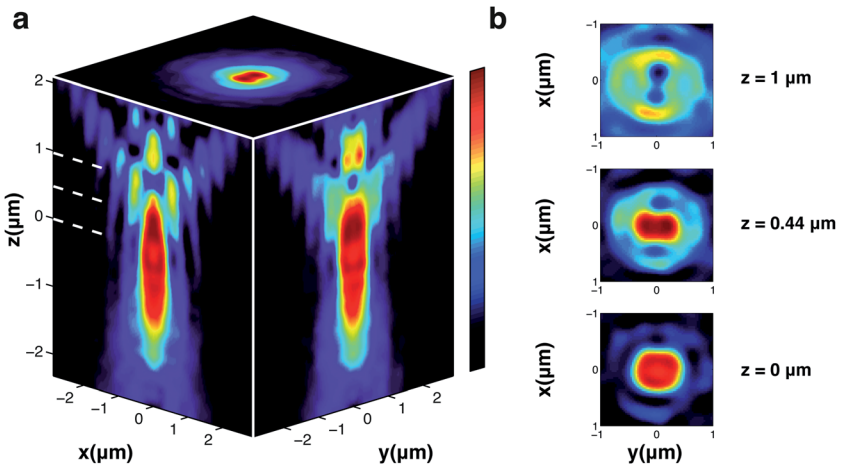

Fig. 4 The 3D focal intensity distribution of the trapping beam (where the laser propagates upwards in the z-direction). (a) Projections of the intensity along the x, y, and z axes, showing an axially asymmetrical intensity distribution. (b) x *versus* y slices along the white dashed lines in (a) showing the intensity at z-heights of ~1.0 μm, ~0.44 μm and at 0 μm; corresponding to the dashed lines in (a).

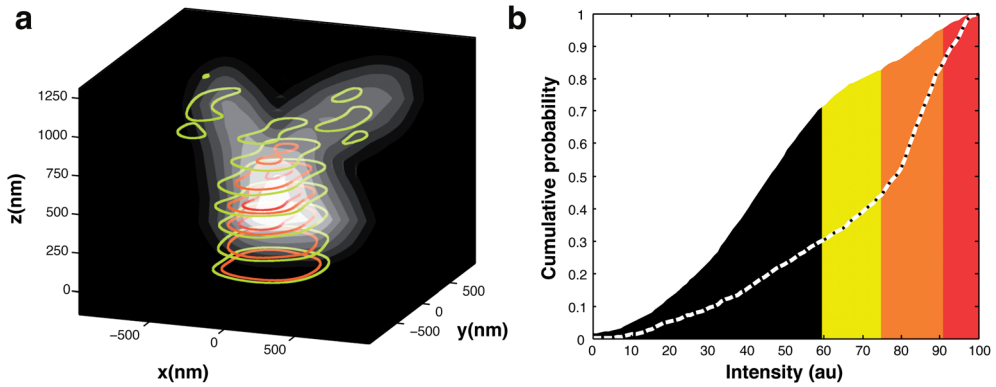

Fig. 5 Comparison of the focal intensity distribution to the positions visited by the trapped QD. (a) Overlay of 3D histogram of positions visited by a colloidal QD (the contours signify 10% steps of the counts) with an intensity contour plot of the focal region. (b) Probability that a trapped QD is located within a region with at least a certain intensity level. The color coding is the same in (a). The black-white dashed line shows an estimate of the accumulated probability of detecting a photon emitted from a QD as function of focal intensity.

positions visited by the trapped QD (Fig. 3c). The trapped QD clearly explores the entire focal region, and also, though relatively seldom, it visits the upward pointing lobes (the 'bunny ears'). In these regions the intensity is relatively low, hence, the likelihood of two-photon exciting the QD is low. This is consistent with the fact that individual QDs are only weakly trapped, hence explore larger parts of the trapping potential compared to large QD aggregates that tend to remain more at the very center of the focus.[13]

An optical trap exerts a harmonic force, F on the trapped particle, in 1D: $F = -\kappa_x x$, where κ_x is the trap stiffness and x is the deviation from the equilibrium position of the particle. The y and z directions are analogous to the x directions albeit with different spring constants, κ_y and κ_z. The thermal fluctuations within the optical trap are well described by the Langevin equation, whose frequency power spectrum yields a Lorentzian function. As shown in ref. 13, the frequency power spectrum of positions visited by a trapped QD is indeed well fitted by a Lorentzian function. The frequency in the power spectrum, which distinguishes the region of confined motion to the region of Brownian fluctuations, is denoted the corner frequency, f_c and it is defined as $f_c = \frac{\kappa_x}{2\pi\gamma}$, where γ is the friction coefficient, given by Stokes law (if far from any surface): $\gamma = 6\pi\eta R$. Here, η denotes the viscosity of the solution and R is the radius of the trapped particle. By fitting a Lorentzian function to the power spectrum of positions visited by the QD, f_c can be found for each dimension.[24] Through knowledge of the hydrodynamic radius ($R = 12$ nm)[25] of the QD also κ_x, κ_y, and κ_z can be determined. One hallmark of optical trapping is that κ_x, κ_y, and κ_z and hence the corresponding corner frequencies, f_c, should be linearly proportional to power, and indeed it was in all three translational directions (as shown in Fig. S2a†).

Assuming the equipartition theorem $\left(\frac{1}{2}\kappa_x\langle x^2\rangle = \frac{1}{2}k_B T\right)$ to be valid we can find the standard deviation of the positions visited, $\sigma_x = \sqrt{\langle x^2\rangle} = \sqrt{\frac{k_B T}{\kappa}}$, where k_B is the Boltzmann constant and T is the temperature. A possible laser induced heating of the trapped QD[26,27] will depend strongly on the laser wavelength and power. To estimate a possible heating of QDs irradiated by our 1064 nm laser we used an assay based on phase-dependent fluorophore partitioning in bilayers.[28–30] This assay directly quantifies the surface temperature of an irradiated nanoparticle and does not require any assumptions about the system, *e.g.*, about the exact intensity at the position of the QD. At the laser powers used, we found the temperature increase to be below the detection threshold of the bilayer assay (below 5 degrees). This is consistent with literature describing the effect of water heating alone.[28,31] Hence, under our experimental conditions the QDs do not heat much and we expect $T = 293$ K is realistic.

The standard deviations of the position histograms decrease with increasing laser power. For a laser power at the sample of 250 mW $\sigma_x = 164 \pm 80$ nm, $\sigma_y = 142 \pm 63$ nm, and $\sigma_z = 141 \pm 60$ nm. From a comparison of these numbers to the extend of the focal region at the same laser power (as visualized in the cross sections of Fig. 4b), it appears a QD mainly moves in a volume that is comparable to the high intensity regions of the focus. Changing the laser power merely changes the extend of the positions visited (as quantified by σ), the shape of the focal volume remains the same. The shape of the focal region will, however, be severely affected by introduction of spherical aberration.[18] Fig. S2b† shows how κ changes with laser power; using the value of κ at 250 mW at the sample and an excursion equal to σ at that laser power, the QD experiences a force of $\sim$0.03 pN.

By analyzing the intensity time series from a two-photon excited QD immobilized on the surface (one example is shown in Fig. 2b) we estimated that the average QD is in a detectable emitting state 3/4 of the time. This estimate is based on the fraction of the time that the QD is detected by the EMCCD detection, there are short-lived dark states which are too short to be detected because of the time resolution of the EMCCD. From analyzing intensity time series from trapped QDs (one example is shown in Fig. 2d) we estimated that emission was detected by the EMCCD from trapped QDs, free to diffuse within the focal volume, only 4% of the total time. If a QD is in a non-emitting dark state 1/4 of the time, then it could have been

within a region with an intensity high enough to render excitation likely ~5% of the time. Fig. 5b shows cumulative probability for a QD to visit the volume with a certain intensity, the curve is almost sinusoidal thus signifying that there is only little probability of finding the QD at the locations with lowest intensity. The part of the curve with the red area under the curve (same color code as in Fig. 5b) shows that the particle is within the 10% most intense part of the focal volume in 5% of the total time, a time that compares well to the excited time observed in Fig. 2d (5%). Within this 10% most intense region we estimate the intensity to be ~16 μJ cm^{-2} s ≈ 6.4 × 10^{25} photons per cm^2 per s.

However, it is probably too simplistic a view that the QD only becomes excited in the most intense region of the focal volume. For two-photon excitation, the excitation probability scales with the intensity squared, hence, there is a possibility of excitation, even within the low intensity regions. To model the situation, we assumed that the probability of excitation would scale with the measured intensity squared at all positions, and the probabilities were normalized to that of the maximum where the intensity was assumed high enough to yield a time trace as depicted in Fig. 2b. The accumulated probability of detecting a QD in an excited state at a certain intensity level is shown in Fig. S3.† In addition, the fact that the detection efficiency of the EMCCD falls off with axial distance to the focus needs to be taken into consideration. To account for this effect, we multiplied the axial intensity distribution with the optical point spread function of the detection system. The resulting accumulated detection probability as function of intensity level is shown in Fig. 5b as a black-white dashed line (and in Fig. S3†). Dipole emitters at a glass surface will exhibit a higher fluorescent intensity compared to emitters in solution, due to radiation patterns skewed towards the glass[33] and CdSe QDs exhibit an increased emission when close to a refractive index interface.[32] At the same time, the excited radiative lifetime of an emitter close to a surface is decreased by the interface[34,35] leading to less blinking. In our samples, the refractive index interface between the coverslip and water will lead to approximately 35–40% higher emission,[35] before considering the lensing effect of the interface. If we also take into account that QDs stuck on the surface are in a dark state 1/4 of the time, this model predicts that QD emission should be observed ~7% of the time while the QD is trapped in solution; this compares well to the experimentally measured 5%.

Elongated quantum dots emit linearly polarized light[36,37] and when optically trapped, they align along the direction of the laser's polarization.[15] However, the 655 QDs used in the present study were close to spherical[38] and probably underwent significant rotational Brownian motion. Hence, an alignment during trapping could not be detected.

Conclusions

We investigated the sub-diffraction dynamics and two-photon excitation of an individual optically trapped colloidal QD. When the QD was two-photon excited for long periods of time, the emission blue-shifted. An optically trapped QD is free to perform Brownian motion within the trap, and its two-photon excited state was observed much more rarely than for a QD stuck in the focus of the laser beam. Using a photodiode we tracked the QD's excursions within all parts of the trapping volume and by translating a fluorescent layer, we mapped the 3D intensity distribution of the focal region. Overlay of these two pieces of information proved that a trapped QD explored all parts of the focal region, also the low-intensity regions, including lobes created by spherical aberration. For this reason, two-photon excitation of a trapped QD could only be detected during a small fraction of the total time trapped. Hence, the optical trapping volume for a colloidal QD is significantly larger than its two-photon excitation volume. For a nanoparticle as a QD, the inherent and unavoidable intensity gradients within a laser focus has huge implications for exactly where the particle will be located and the likelihood of two-photon excitation, hence, these results are important for realization of nano-scale optical control and visualization of a QD.

Acknowledgements

We thank C. B. Lagerholm and MEMPHYS for lending us the QuadView image splitter and H. Ma for experimental assistance. We acknowledge financial support from the Carlsberg Foundation, the Lundbeck Foundation, and from the University of Copenhagen Excellence Program.

References

1 W. C. W. Chan and S. M. Nie, *Science*, 1998, **281**, 2016–2018.
2 X. Michalet, F. Pinaud, T. D. Lacoste, M. Dahan, M. P. Bruchez, A. P. Alivisatos and S. Weiss, *Single Mol.*, 2001, **2**, 261–276.
3 X. Michalet, F. F. Pinaud, L. A. Bentolila, J. M. Tsay, S. Doose, J. J. Li, G. Sundaresan, A. M. Wu, S. S. Gambhir and S. Weiss, *Science*, 2005, **307**, 538–544.
4 Y. Ebenstein, N. Gassman, S. Kim, J. Antelman, Y. Kim, S. Ho, R. Samuel, X. Michalet and S. Weiss, *Nano Lett.*, 2009, **9**, 1598–1603.
5 I. J. Finkelstein, M.-L. Visnapuu and E. C. Greene, *Nature*, 2010, **1**, 1–5.
6 R. Edgar, A. Rokney, M. Feeney, S. Semsey, M. Kessel, M. B. Goldberg, S. Adhya and A. B. Oppenheim, *Mol. Microbiol.*, 2008, **68**, 1107–1116.
7 B. Dubertret, P. Skourides, D. J. Norris, V. Noireaux, A. H. Brivanlou and A. Libchaber, *Science*, 2002, **298**, 1759–1762.
8 A. Biebricher, W. Wende, C. Escude, A. Pingoud and P. Desbiolles, *Biophys. J.*, 2009, **96**, L50–L52.
9 M. Eriksen, P. Horvath, M. A. Sørensen, S. Semsey, L. B. Oddershede and L. Jauffred, *J. Nanomater.*, 2013, **2013**, 1–9.
10 D. M. Warshaw, G. G. Kennedy, S. S. Work, E. B. Krementsova, S. Beck and K. M. Trybus, *Biophys. J.*, 2005, **88**, L30–L32.
11 A. Seitz and T. Surrey, *EMBO J.*, 2006, **25**, 267–277.

12 M. Dahan, S. Levi, C. Luccardini, P. Rostaing, B. Riveau and A. Triller, *Science*, 2003, **302**, 442–445.
13 L. Jauffred, A. C. Richardson and L. B. Oddershede, *Nano Lett.*, 2008, **8**, 3376–3380.
14 L. Jauffred and L. B. Oddershede, *Nano Lett.*, 2010, **10**, 1927–1930.
15 C. R. Head, E. Kammann, M. Zanella, L. Manna and P. G. Lagoudakis, *Nanoscale*, 2012, **4**, 3693–3697.
16 S. Reihani, H. Khalesifard and R. Golestanian, *Opt. Commun.*, 2006, **259**, 204–211.
17 S. N. S. Reihani and L. B. Oddershede, *Opt. Lett.*, 2007, **32**, 1998–2000.
18 A. Kyrsting, P. M. Bendix and L. B. Oddershede, *Nano Lett.*, 2013, **13**, 31–35.
19 T. Čižmár, M. Mazilu and K. Dholakia, *Nat. Photonics*, 2010, **4**, 388–394.
20 E. Arnspang Christensen, P. Kulatunga and B. C. Lagerholm, *PLoS One*, 2012, **7**, e44355.
21 B. R. Fisher, N. E. Stott and M. G. Bawendi, *J. Phys. Chem. B*, 2004, **11**, 143–148.
22 M. Pelton, G. Smith, N. F. Scherer and R. A. Marcus, *Proc. Natl. Acad. Sci. U. S. A.*, 2007, **104**, 14249–14254.
23 C. Hosokawa, H. Yoshikawa and H. Masuhara, *Phys. Rev. E: Stat., Nonlinear, Soft Matter Phys.*, 2005, **72**, 1–7.
24 P. M. Hansen, I. M. Tolic-Nørrelykke, H. Flyvbjerg and K. Berg-Sørensen, *Comput. Phys. Commun.*, 2006, **175**, 572–573.
25 E. C. Arnspang, J. R. Brewer and B. C. Lagerholm, *PLoS One*, 2012, **7**, e48521.
26 P. Haro-González, B. del Rosal, L. M. Maestro, E. M. Rodríguez, R. Naccache, J. a. Capobianco, K. Dholakia, J. G. Solé and D. Jaque, *Nanoscale*, 2013, **5**, 12192–12199.
27 P. Haro-González, W. T. Ramsay, L. Martinez Maestro, B. del Rosal, K. Santacruz-Gomez, M. D. C. Iglesias-de la Cruz, F. Sanz-Rodríguez, J. Y. Chooi, P. Rodriguez Sevilla, M. Bettinelli, D. Choudhury, A. K. Kar, J. G. Solé, D. Jaque and L. Paterson, *Small*, 2013, **9**, 2162–2170.
28 P. M. Bendix, S. N. S. Reihani and L. B. Oddershede, *ACS Nano*, 2010, **4**, 2256–2262.
29 H. Ma, P. M. Bendix and L. B. Oddershede, *Nano Lett.*, 2012, **12**, 3954–3960.
30 H. Ma, P. Tian, J. Pello, P. M. Bendix and L. B. Oddershede, *Nano Lett.*, 2014, **14**, 612–619.
31 E. J. Peterman, F. Gittes and C. F. Schmidt, *Biophys. J.*, 2003, **84**, 1308–1316.
32 X. Brokmann, L. Coolen, J.-P. Hermier and M. Dahan, *Chem. Phys.*, 2005, **318**, 91–98.
33 W. Lukosz, *J. Opt. Soc. Am.*, 1979, **69**, 1495–1503.
34 W. Lukosz and R. E. Kunz, *J. Opt. Soc. Am.*, 1977, **67**, 1607–1615.
35 W. Lukosz and R. E. Kunz, *Opt. Commun.*, 1977, **20**, 195–199.
36 J. Hu, L. Ls, W. Yang, L. Manna, W. Lw and A. P. Alivisatos, *Science*, 2001, **292**, 2060–2063.
37 V. Kulakovskii, G. Bacher, R. Weigand, T. Kümmell, A. Forchel, E. Borovitskaya, K. Leonardi and D. Hommel, *Phys. Rev. Lett.*, 1999, **82**, 1780–1783.
38 L. Jauffred, M. Sletmoen, F. Czerwinski and L. B. Oddershede, *Proc. SPIE*, 2010, **7762**, 776226.